

## Effect of a post-deposition anneal on Al<sub>2</sub>O<sub>3</sub>/Si interface properties

J. Benick<sup>1</sup>, A. Richter<sup>1</sup>, T. T. A. Li<sup>3</sup>, N. E. Grant<sup>2</sup>, K. R. McIntosh<sup>2</sup>, Y. Ren<sup>2</sup>, K. J. Weber<sup>2</sup>, M. Hermle<sup>1</sup>, S. W. Glunz<sup>1</sup>

<sup>1</sup>Fraunhofer Institute for Solar Energy Systems (ISE), Heidenhofstrasse 2, D-79110 Freiburg, Germany

<sup>2</sup>Centre for Sustainable Energy Systems, The Australian National University, Canberra, ACT 0200, Australia

<sup>3</sup>School of Engineering, The Australian National University, Canberra, ACT 0200, Australia

### ABSTRACT

While Al<sub>2</sub>O<sub>3</sub> has been proven to provide an excellent level of surface passivation on all sorts of p-type doped silicon surfaces, the passivation mechanism of this layer and especially the influence of the post-deposition anneal on the Al<sub>2</sub>O<sub>3</sub>/Si interface properties is not yet completely understood. A great increase in the surface passivation is observed after a post-deposition anneal, i.e. a post-deposition anneal is mandatory to activate the surface passivation. Thus, the influence of this anneal on the interface properties, density of negative fixed charges Q<sub>f</sub> and density of interface traps D<sub>it</sub>, will be investigated and correlated to the measured minority carrier lifetime. In the case of plasma enhanced ALD, Q<sub>f</sub> is already high in the as-deposited state and the annealing process only has a minor effect on Q<sub>f</sub> (Q<sub>f</sub> increases by 20-50 %, depending on the annealing temperature). The D<sub>it</sub> however is strongly reduced by the post-deposition anneal, decreasing by two orders of magnitude. This large reduction in D<sub>it</sub> is a prerequisite for benefiting from the strong field effect induced by the high density of negative charges of the Al<sub>2</sub>O<sub>3</sub>.

### INTRODUCTION

In recent years Al<sub>2</sub>O<sub>3</sub> has been proven to be capable of providing an excellent passivation on all sorts of p-type doped surfaces [1, 2]. Especially in photovoltaics this closes a gap, as an effective low-temperature passivation on p-type surfaces was missing in the past. A first application is the reduction of the surface recombination at the rear side of p-type silicon solar cells. For this purpose Al<sub>2</sub>O<sub>3</sub> is a promising alternative to thermally grown SiO<sub>2</sub>. On p-type PERC solar cells several authors showed that Al<sub>2</sub>O<sub>3</sub> is at least as effective for the rear side passivation as thermally grown, annealed SiO<sub>2</sub> [3, 4]. Furthermore the realization of alternative solar cell concepts, e.g. on n-type silicon, might be enabled by the application of Al<sub>2</sub>O<sub>3</sub> as well. Due to the effective passivation of the front side boron emitter by Al<sub>2</sub>O<sub>3</sub>, we were able to realize conversion efficiencies of 23.5% on n-type PERL solar cells. Thus, the properties of the Al<sub>2</sub>O<sub>3</sub> passivation using different deposition techniques (ALD, PECVD, rf sputtering) are being investigated by various authors [5-10]. However, the passivation mechanism of Al<sub>2</sub>O<sub>3</sub> is not yet completely understood. In general, two different strategies for the passivation of surfaces, i.e. the reduction of the surface recombination, exist: (i) reduction of the interface trap density (D<sub>it</sub>) and (ii) field effect passivation due to fixed charges (Q<sub>f</sub>) within the dielectric passivation layer.

Particularly a very high density of fixed negative charges, Q<sub>f</sub>, (up to  $\sim 10^{13} \text{ cm}^{-3}$ ) is one of the special characteristics of the Al<sub>2</sub>O<sub>3</sub>. However, to be able to reach a high level of surface passivation as is reported for Al<sub>2</sub>O<sub>3</sub>, in addition to an effective field effect passivation, the density of interface traps has to be greatly reduced as well. Indeed, low densities of interface traps, D<sub>it</sub>, in the range of  $\sim 8 \times 10^{10}$  to  $2 \times 10^{11} \text{ cm}^{-2} \text{ eV}^{-1}$  are reported [6, 11]. However, in the as-deposited state, no passivation is provided by the Al<sub>2</sub>O<sub>3</sub> at all, regardless of the deposition method. An additional post-deposition anneal is required to activate the surface passivation. In practice the initial carrier lifetime of 1  $\mu\text{s}$  increases to  $> 2 \text{ ms}$  after annealing at 425°C (1  $\Omega \text{ cm}$  p-type FZ-Si). Thus, substantial changes in the Al<sub>2</sub>O<sub>3</sub> layer itself or at the silicon interface occur during the post deposition anneal. The influence of this post-deposition anneal on the Al<sub>2</sub>O<sub>3</sub>/Si interface properties (density of negative fixed charges Q<sub>f</sub> as well as on the density of interface traps D<sub>it</sub>) is investigated within this work and will be correlated to the measured minority carrier lifetime. A thin ( $\sim 1\text{--}2 \text{ nm}$ ) layer of SiO<sub>x</sub> is often observed to be present at the silicon interface or to develop during the anneal process [1, 12], i.e. an Al<sub>2</sub>O<sub>3</sub>/SiO<sub>x</sub>-Si interface. In the following, however, the interface will be referred to as Al<sub>2</sub>O<sub>3</sub>/Si.

### EXPERIMENTAL

For the investigation of the Al<sub>2</sub>O<sub>3</sub>/Si interface properties MIS (metal/insulator/semiconductor) capacitor structures were prepared on shiny etched 1  $\Omega \text{ cm}$  p-type FZ Si(100) substrates with a thickness of 250  $\mu\text{m}$ . D<sub>it</sub> and Q<sub>f</sub> of the MIS samples were determined by high-frequency and quasistatic capacitance-voltage (C-V) measurements [13]. To measure the effective minority carrier lifetime ( $\tau_{\text{eff}}$ ), symmetrically coated lifetime samples have been processed on the same substrate material. These samples were characterized by the Quasi Steady State PhotoConductance (QSSPC) method [14]. From these lifetime measurements the maximum effective surface recombination velocity S<sub>eff</sub> was determined by [15]

$$\frac{1}{\tau_{\text{eff}}} = \frac{1}{\tau_{\text{bulk}}} + \frac{1}{W / (2S_{\text{eff}}) + W^2 / (D\pi^2)} \quad (1)$$

with W the wafer thickness and D the minority charge carrier diffusion constant. Assuming an infinite bulk lifetime  $\tau_{\text{bulk}}$ , we therefore determine an upper limit to S<sub>eff</sub>. To get some information of a possible change in the layer composition by the annealing process FTIR

measurements have been performed on the symmetrically coated lifetime samples as well.

The dielectric passivation layer  $\text{Al}_2\text{O}_3$  (30 nm) was deposited by PE-ALD (OpAL™, Oxford instruments) at a temperature of 180°C. Prior to the  $\text{Al}_2\text{O}_3$  deposition the samples were cleaned by a  $\text{HNO}_3$  etch followed by a short HF (1%) dip. The samples then underwent a 25 min post-deposition anneal on a hotplate in ambient atmosphere at a temperature ranging from 300°C to 550°C. For the MIS structure aluminium dots (700 µm) were thermally evaporated through a shadow mask. Eutectic gallium-indium was used to ensure a good rear side contact of the MIS structure.

## RESULTS AND DISCUSSION

The measured injection-level-dependent minority carrier lifetime of the lifetime samples which were coated on both sides with  $\text{Al}_2\text{O}_3$  in Figure 1 shows an extreme influence of the post deposition anneal on the  $\text{Al}_2\text{O}_3$  surface passivation. Whereas in the as-deposited state with a measured lifetime of  $\sim 1 \mu\text{s}$  no passivation at all is provided by the  $\text{Al}_2\text{O}_3$ , the measured lifetime increases with increasing annealing temperature up to  $\sim 2.3 \text{ ms}$ , a value close to the Auger-limit [16], at a temperature of  $\sim 425^\circ\text{C}$ . For higher annealing temperatures above 425°C the lifetime decreases again. However, this decrease is only small, after annealing at 550°C the lifetime is still well above 1 ms (1.2 ms @  $\Delta n = 10^{15} \text{ cm}^{-3}$ ).

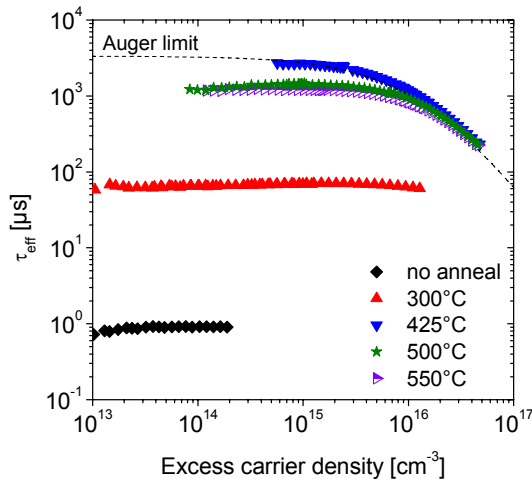


**Figure 1** Injection-dependent minority carrier lifetime of the PE-ALD  $\text{Al}_2\text{O}_3$  passivated lifetime samples in the as-deposited state as well as after annealing (hotplate) at different temperatures.

To relate this strong dependence of the passivation quality of the  $\text{Al}_2\text{O}_3$  passivation on the post deposition anneal to the interface properties, MIS structures were measured with C-V techniques. Figure 2 shows the high-frequency and quasistatic C-V curves of the PE-ALD  $\text{Al}_2\text{O}_3$

passivated MIS samples for different post deposition annealing temperatures.

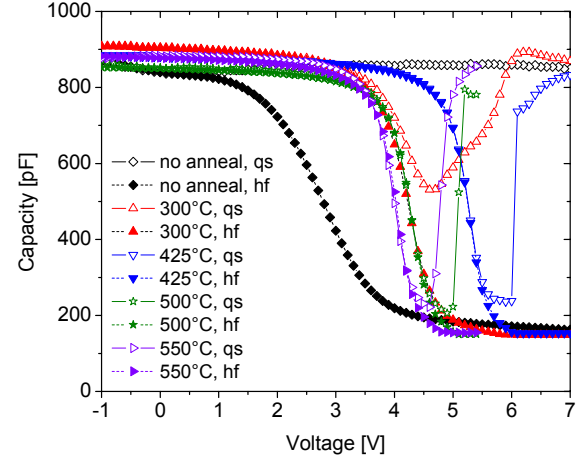


**Figure 2** High-frequency (hf) and quasistatic (qs) capacitance-voltage measurements of PE-ALD  $\text{Al}_2\text{O}_3$  passivated MIS samples ( $1 \Omega \text{ cm } p\text{-type FZ}$ ) after post-deposition anneal (hotplate) at different temperatures.

The accumulation and inversion capacitance of all four MIS structures is consistent with the values expected of such samples. The accumulation capacitance assumed equal to the insulator capacitance, is measured to be  $C_{\text{insulator}} = 880 \pm 30 \text{ pF}$ , which amounts to the  $\text{Al}_2\text{O}_3$  having a dielectric constant of  $8.1 \pm 0.3$ , as calculated from the area of the metal ( $A = 0.0038 \text{ cm}^2$ ) and the thickness of the  $\text{Al}_2\text{O}_3$  ( $t_{\text{insulator}} = 30 \text{ nm}$ ), from

$$\varepsilon_i = \frac{C_{\text{insulator}} t_{\text{insulator}}}{A}. \quad (2)$$

While the accumulation and inversion capacitance are similar for all four MIS structures, the C-V curves also exhibit pronounced differences in relation to (i) translation on the X-axis due to charge in the dielectric; (ii) the difference between quasistatic and high frequency curves due to the interface states; and (iii) "stretch-out", also due to interface states [13].

The fixed charge in the dielectric layer,  $Q_f$ , can be determined from the flatband voltage,  $V_{fb}$ , (neglecting the influence of  $Q_{it}$ ) from the high-frequency C-V curve by

$$Q_f = (\Phi_{ms} - V_{fb}) C_{\text{insulator}} \quad (3)$$

with  $\Phi_{ms}$  being the difference between the metal and silicon work functions, and where  $Q_f$  is assumed to reside at the  $\text{Al}_2\text{O}_3/\text{Si}$  interface. The flatband voltage increases from 2.8 V in the as-deposited state up to 4.9 V at an annealing temperature of 425°C, the charge densities are  $-6.0 \times 10^{12} \text{ cm}^{-2}$  and  $-9.9 \times 10^{12} \text{ cm}^{-2}$  respectively. For higher

post-deposition annealing temperatures the shift in the flatband voltage is smaller, and thus  $Q_f$  is comparatively smaller in magnitude as well (see Fig. 3a). A number of methods are available for extracting the density of interface states  $D_{it}$ . One of the more accurate and very common methods for the extraction of  $D_{it}$  is based on the comparison of the high-frequency and quasistatic C-V curve (Castagne and Vapaille [17]). The smaller the difference between the two C-V curves, the lower is the density of interface traps. Thus, by regarding the original curves it can be qualitatively stated that the  $D_{it}$  decreases with increasing temperature of the post-deposition anneal. We have used three different methods to determine  $D_{it}$ : (i) from the high-frequency [18], (ii) from the quasistatic [19] and (iii) from the comparison of high-frequency and quasistatic C-V curves [17]. An overview over the data extracted from the C-V curves ( $Q_f$ ,  $D_{it}$  at midgap) as well as the respective minority carrier lifetimes (at  $\Delta n = 10^{15} \text{ cm}^{-3}$ ) is shown in Figure 3. As mentioned earlier, up to  $\sim 425^\circ\text{C}$  the density of negative charges increases with increasing temperature of the post-deposition anneal and decreases again for higher temperatures. In general, with a value of  $-6.0 \times 10^{12} \text{ cm}^{-2}$  already in the as-deposited state the density of negative charges is relatively high. The increase of the charge density, due to the post deposition anneal, therefore only corresponds to a factor of 1.6.  $D_{it}$  at midgap however decreases with increasing post deposition annealing temperature by two orders of magnitude. In the as-deposited state, due to the flat progression of the quasistatic C-V curve, the  $D_{it}$  could only be extracted from the high-frequency C-V curve. With a value of  $\sim 3 \times 10^{13} \text{ cm}^{-2} \text{ eV}^{-1}$  at midgap, the  $D_{it}$  in the as-deposited state is very high. However, by the post deposition annealing this high  $D_{it}$  can be lowered by approximately two orders of magnitude, to  $\sim 1.3 \times 10^{11} \text{ cm}^{-2} \text{ eV}^{-1}$  at midgap, by annealing at a temperature of  $500^\circ\text{C}$ . The different methods for the extraction of  $D_{it}$  here result in comparable  $D_{it}$  values, suggesting a reliable  $D_{it}$  measurements. Regarding the measured minority carrier lifetime, shown in Fig. 3c, it can be seen that the lifetime varies by orders of magnitude as well. The increase of the minority carrier lifetime with increasing annealing temperature (up to  $425^\circ\text{C}$ ) thus can be related to the improvement of the interface, i.e. the reduction of the density of interface traps. This becomes particularly obvious by the comparison of the samples annealed at  $300^\circ\text{C}$  and  $500^\circ\text{C}$ . Those samples having a comparable density of negative interface charges ( $Q_{f,300} = -8.2 \times 10^{12} \text{ cm}^{-2}$  and  $Q_{f,500} = -8.3 \times 10^{12} \text{ cm}^{-2}$  respectively,  $Q_{f,500}/Q_{f,300} = 1.02$ ), show a pronounced difference in the density of interface traps of more than one order of magnitude ( $D_{it,300}/D_{it,500} = 26.0$ ). Thus, as the density of fixed charges of these samples is nearly the same and the effective surface recombination velocity is proportional to  $D_{it}$ , the ratio  $S_{eff,300}/S_{eff,500}$  should be the same as  $D_{it,300}/D_{it,500}$ . In fact, taking the quotient  $S_{eff,300}/S_{eff,500}$  this results in a value of 22.1, which is close to the value that has been calculated for  $D_{it,300}/D_{it,500}$  (26.0). Thus, it can be stated, that the great improvement of the surface passivation of the  $\text{Al}_2\text{O}_3$  by a post-

deposition anneal is mainly related to the reduction of  $D_{it}$ . A sufficiently low level of  $D_{it}$  therefore is necessary to benefit from the field effect induced by the negative interface charges.

It has already been reported that a density of negative charges in the range of  $-5 \times 10^{12} \text{ cm}^{-2}$  is sufficient for an effective field effect passivation [20, 21]. Higher charge densities therefore only lead to modest improvements of the passivation. This is also confirmed by the samples annealed at  $425^\circ\text{C}$  and  $500^\circ\text{C}$ , which have almost identical values for  $D_{it}$ . The effect of the different charge densities ( $-9.9 \times 10^{12} \text{ cm}^{-2}$  and  $-8.3 \times 10^{12} \text{ cm}^{-2}$ ) of these samples is only moderate (2660  $\mu\text{s}$  and 1460  $\mu\text{s}$  respectively).

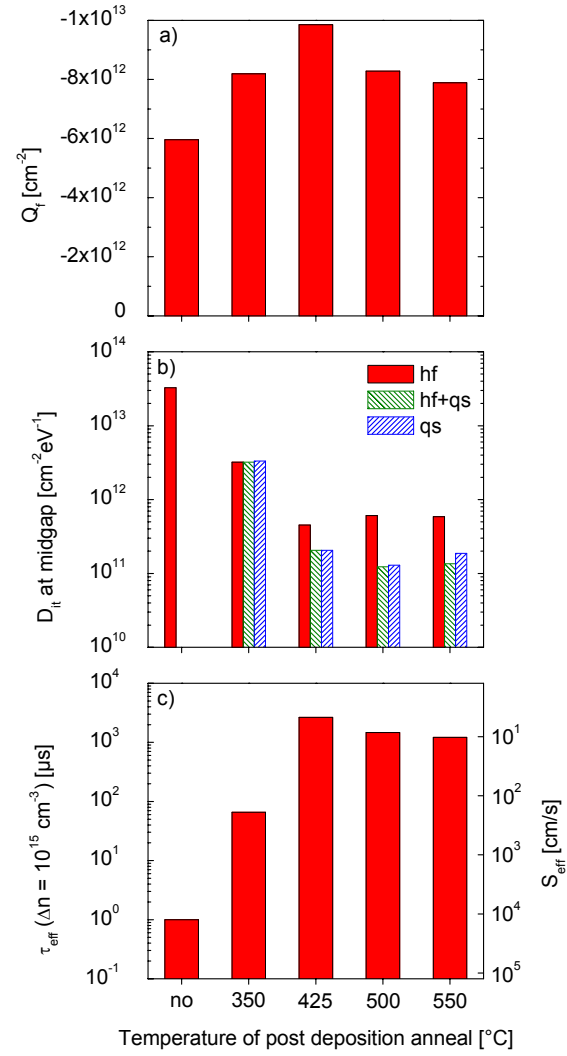


**Figure 3** Charge density ( $Q_f$ ), interface defect density ( $D_{it}$ ) at midgap and effective lifetime ( $\tau_{eff}$ ) of the annealed samples passivated by PE-ALD  $\text{Al}_2\text{O}_3$ .  $Q_f$  and  $D_{it}$  were extracted from the C-V data,  $\tau_{eff}$  was measured on identically processed lifetime samples (1  $\Omega$  cm p-type FZ Si).

These observed significant changes in the interface properties indicate that substantial changes in the physical  $\text{Al}_2\text{O}_3/\text{Si}$  interface occur. For non-annealed  $\text{Al}_2\text{O}_3$  layers, i.e. in the as-deposited state, different observations have been reported. An abrupt interface between  $\text{Al}_2\text{O}_3$  and Si is reported for  $\text{Al}_2\text{O}_3$  layers deposited by low pressure MOCVD and thermal ALD [12, 22]. For plasma assisted ALD deposited  $\text{Al}_2\text{O}_3$  layers however a thin (1.2 nm) interfacial  $\text{SiO}_x$  is reported [1], that has been attributed to the exposure of the substrate to the  $\text{O}_2$  plasma during the first ALD cycles. An annealing process however leads to the formation of a thin interfacial  $\text{SiO}_x$ , independent of the initial interface [1, 12]. The interfacial  $\text{SiO}_2$  layer is supposed to play a central role with respect to the  $\text{Al}_2\text{O}_3$  surface passivation. Johnson *et al.* [23] and Kimoto *et al.* [24] have already shown that an interfacial  $\text{SiO}_2$  is crucial for the formation of the negative interface charges. Further,  $\text{SiO}_2$  is known to effectively reduce the  $D_{it}$  at the  $\text{SiO}_2/\text{Si}$  interface [25]. Thus, such a thin interfacial  $\text{SiO}_2$  might be responsible for the low  $D_{it}$  of the  $\text{Al}_2\text{O}_3$  passivation after the post-deposition anneal.

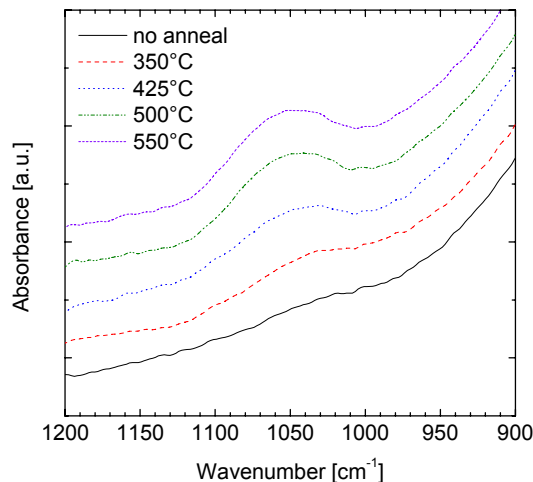


**Figure 4 FTIR spectra of the ALD  $\text{Al}_2\text{O}_3$  passivated samples annealed at different temperatures. After annealing the peak related to the asymmetric stretch of the O in Si-O-Si bridging bonds can be observed and increases with increasing annealing temperature.**

The FTIR measurements that were performed on the  $\text{Al}_2\text{O}_3$  passivated lifetime samples with increasing annealing temperature show the evolution of an absorption band at  $1060 \text{ cm}^{-1}$ . This absorption band is known to originate from the TO mode arising from the asymmetric stretching of O in Si-O-Si in thermally grown amorphous silicon dioxide (a- $\text{SiO}_2$ ) [26, 27]. Thus, this indicates that for the annealed samples an interfacial  $\text{SiO}_2$  layer exists between the  $\text{Al}_2\text{O}_3$  and the silicon substrate. However for the as-deposited sample this absorption band cannot be observed, indicating a different chemical configuration or even a non-existence of an intermediate  $\text{SiO}_2$  layer. Thus, by the correlation to the measured

effective lifetime as well as the  $D_{it}$  it can be stated that the interfacial  $\text{SiO}_x$  plays a central role in the passivation of silicon surfaces by  $\text{Al}_2\text{O}_3$ .

## SUMMARY

In summary, the  $\text{Al}_2\text{O}_3/\text{Si}$  interface properties,  $D_{it}$  and  $Q_f$  have been measured as a function of the temperature of the post-deposition annealing and have been correlated to the minority carrier lifetime. Both,  $Q_f$  and  $D_{it}$  are affected by the post deposition anneal. However, even in the as-deposited state the PE-ALD deposited  $\text{Al}_2\text{O}_3$  shows a sufficiently high density of negative charges and the impact of the annealing on the charge density is only moderate. From C-V measurements,  $Q_f$  increases from  $-6.0 \times 10^{12} \text{ cm}^{-2}$  in the as-deposited state to  $-9.9 \times 10^{12} \text{ cm}^{-2}$  after annealing at a temperature of  $425^\circ\text{C}$  ( $Q_{f,425}/Q_{f,\text{as-dep}} = 1.6$ ). The initially high  $D_{it}$  at midgap, however is strongly reduced (two orders of magnitude) with increasing temperature of the post deposition annealing up to  $550^\circ\text{C}$ . The minority carrier lifetime at the same time increases from  $1 \mu\text{s}$  in the as deposited state to  $>2 \text{ ms}$  after annealing at  $425^\circ\text{C}$ . Thus the great improvement of the  $\text{Al}_2\text{O}_3$  surface passivation by the post deposition annealing is mainly related to the strong improvement of the  $D_{it}$  at the  $\text{Al}_2\text{O}_3/\text{Si}$  interface. A sufficiently low  $D_{it}$  therefore is a prerequisite to benefit from the strong field effect induced by the high density of negative charges of the  $\text{Al}_2\text{O}_3$ . FTIR measurements indicate that a thin interfacial layer of  $\text{SiO}_2$  is formed during the annealing process. This interfacial  $\text{SiO}_2$  layer is supposed to play a central role with respect to the  $\text{Al}_2\text{O}_3$  surface passivation and further investigations have to be performed to examine the function of this layer on a microscopic scale.

## ACKNOWLEDGEMENT

J. B. acknowledges the DAAD for financial support. The work was supported by the German Federal Ministry for the Environment, Nature Conservation and Nuclear Safety under contract number 0329849A "Th-ETA".

## REFERENCES

- [1] B. Hoex, S.B.S. Heil, E. Langereis, M.C.M. van de Sanden and W.M.M. Kessels, "Ultralow surface recombination of c-Si substrates passivated by plasma-assisted atomic layer deposited  $\text{Al}_2\text{O}_3$ ", Applied Physics Letters **89** (2006) 042112.
- [2] B. Hoex, J. Schmidt, R. Bock, P.P. Altermatt, M.C.M. van de Sanden, et al., "Excellent passivation of highly doped p-type Si surfaces by the negative-charge-dielectric  $\text{Al}_2\text{O}_3$ ", Applied Physics Letters **91** (2007) 112107.
- [3] P. Saint-Cast, J. Benick, D. Kania, L. Weiss, M. Hofmann, et al., "High-Efficiency c-Si Solar Cells Passivated With ALD and PECVD Aluminum Oxide", Electron Device Letters, IEEE (2010) DOI: 10.1109/LED.2010.2049190

- [4] J. Schmidt, A. Merkle, R. Brendel, B. Hoex, M.C.M. van de Sanden, et al., "Surface passivation of high-efficiency silicon solar cells by atomic-layer-deposited Al<sub>2</sub>O<sub>3</sub>", *Progress in Photovoltaics: Research and Applications* **16** (2008) 461.
- [5] S. Miyajima, J. Irikawa, A. Yamada and M. Konagai, "Hydrogenated Aluminum Oxide Films Deposited by Plasma Enhanced Chemical Vapor Deposition For Passivation of P-Type Cystalline Silicon", *Proceedings of the 23rd European Photovoltaic Solar Energy Conference*, Valencia, Spain (2008) 1029.
- [6] P. Saint-Cast, D. Kania, M. Hofmann, J. Benick, J. Rentsch, et al., "Very low surface recombination velocity on p-type c-Si by high rate plasma-deposited aluminum oxide", *Applied Physics Letters* **95** (2009) 151502.
- [7] T.-T. Li and A. Cuevas, "Effective Surface Passivation of Crystalline Silicon by RF Sputtered Aluminum Oxide", *Physica Status Solidi RRL* **3** (2009) 160.
- [8] G. Dingemans, P. Engelhart, R. Seguin, B. Hoex, M.C.M. van de Sanden, et al., "Firing Stability of Atomic Layer Deposited Al<sub>2</sub>O<sub>3</sub> for C-Si Surface Passivation", *Proceedings of the 34th IEEE Photovoltaics Specialists Conference*, Philadelphia, Pennsylvania, USA (2009).
- [9] J. Schmidt, B. Veith and R. Brendel, "Effective surface passivation of crystalline silicon using ultrathin Al<sub>2</sub>O<sub>3</sub> films and Al<sub>2</sub>O<sub>3</sub>/SiNx stacks", *Physica Status Solidi RRL* **3** (2009) 287.
- [10] J. Benick, A. Richter, M. Hermle and S.W. Glunz "Thermal stability of the Al<sub>2</sub>O<sub>3</sub> passivation on p-type silicon surfaces for solar cell application", *Physica Status Solidi RRL* **3** (2009) 233.
- [11] R. Hezel and K. Jaeger, "Low-temperature surface passivation of silicon for solar cells", *Journal of the Electrochemical Society* **136** (1989) 518.
- [12] A.R. Chowdhuri and C.G. Takoudis, "Investigation of the aluminium oxide/Si(100) interface formed by chemical vapor deposition", *Thin Solid Films* **446** (2004) 155.
- [13] E.H. Nicollian and J.R. Brews, *MOS Physics and Technology*, Wiley, New York (1982).
- [14] R.A. Sinton, A. Cuevas and M. Stuckings, "Quasi-steady-state photoconductance, a new method for solar cell material and device characterization", *Proceedings of the 25th IEEE Photovoltaic Specialists Conference*, Washington DC, USA (1996) 457.
- [15] A.B. Sproul, "Dimensionless solution of the equation describing the effect of surface recombination on carrier decay in semiconductors", *Journal of Applied Physics* **76** (1994) 2851.
- [16] M.J. Kerr and A. Cuevas, "General parameterization of Auger recombination in crystalline silicon", *Journal of Applied Physics* **91** (2002) 2473.
- [17] R. Castagne and A. Vapaille, "Description of the SiO<sub>2</sub>-Si interface properties by means of very low frequency MOS capacitance measurements", *Surface Science* **28** (1971) 157.
- [18] L.M. Terman, "An investigation of surface states at a Silicon/Silicon oxide interface employing Metal-Oxide-Silicon diodes", *Solid State Electronics* **5** (1962) 285.
- [19] C.N. Berglund, "Surface states at steam grown Silicon dioxide interfaces", *IEEE Transaction on Electron Devices* **13** (1966) 701.
- [20] J. Benick, B. Hoex, M.C.M. van de Sanden, W.M.M. Kessels, O. Schultz, et al., "High efficiency n-type Si solar cells on Al<sub>2</sub>O<sub>3</sub>-passivated boron emitters", *Applied Physics Letters* **92** (2008) 253504.
- [21] W. Jellett, "Investigation of Recombination at the Silicon-Silicon Dioxide Interface", *Dissertation, Australian National University*, (2008)
- [22] E.P. Gusev, M. Copel and E. Cartier, "High-resolution depth profiling in ultrathin Al<sub>2</sub>O<sub>3</sub> films on Si", *Applied Physics Letters* **76** (2000) 176.
- [23] R.S. Johnson, G. Lucovsky and I. Baumvol, "Physical and Electrical Properties of Noncrystalline Al<sub>2</sub>O<sub>3</sub> Prepared by Remote Plasma Enhanced Chemical Vapor Deposition", *J. Vac. Sci. Technol. A* **19** (2001) 1353.
- [24] K. Kimoto, Y. Matsui, T. Nabatame, T. Yasuda, T. Mizoguchi, et al., "Coordination and Interface Analysis of Atomic-Layer-Deposition Al<sub>2</sub>O<sub>3</sub> on Si(001) Using Energy-Loss Near-Edge Structures", *Applied Physics Letters* **83** (2003) 4306.
- [25] A.G. Aberle, S. Glunz and W. Warta, "Impact of illumination level and oxide parameters on Shockley-Read-Hall recombination at the Si-SiO<sub>2</sub> interface", *Journal of Applied Physics* **71** (1992) 4422.
- [26] C.T. Kirk, "Quantitative analysis of the effect of disorder-induced mode coupling on infrared absorption in silica", *Physical Review B* **38** (1988) 1255.
- [27] K.T. Queeney, M.K. Weldon, J.P. Chang, Y.J. Chabal, A.B. Gurevich, et al., "Infrared spectroscopic analysis of the Si/SiO<sub>2</sub> interface structure of thermally oxidized silicon", *Journal of Applied Physics* **87** (2000) 1322.